AFCRL-63-254

DESIGN HISTORY AND THEORY OF OPERATION OF A TWO-CHANNEL, ROCKET-BORNE EBERT GRATING SPECTROMETER

by

Merle J. Persky
Eugene K. Dana
Geert Wyntjes

Scientific Report No. 5
Contract No. AF 19(604)-5738
ARPA Order 30-60
Project No. 4094
Task No. 49045

January 9, 1963

Prepared for
Geophysics Research Directorate
Air Force Cambridge Research Laboratories
Air Research and Development Command
United States Air Force
Bedford, Massachusetts

Block Associates, Inc.
CAMBRIDGE 39, MASSACHUSETTS

63. 3. 3

AFCRL-63-254

DESIGN HISTORY AND THEORY OF OPERATION OF A TWO-CHANNEL, ROCKET-BORNE EBERT GRATING SPECTROMETER

by

Merle J. Persky
Eugene K. Dana
Geert Wyntjes

Scientific Report No. 5
Contract No. AF 19(604)-5738
ARPA Order 30-60
Project No. 4094
Task No. 49045

January 9, 1963

Prepared for
Geophysics Research Directorate
Air Force Cambridge Research Laboratories
Air Research and Development Command
United States Air Force
Bedford, Massachusetts

Block Associates, Inc.
CAMBRIDGE 39, MASSACHUSETTS

Requests for additional copies by Agencies of the Department of Defense, their contractors, and other Government agencies should be directed to the:

ARMED SERVICES TECHNICAL INFORMATION AGENCY
ARLINGTON HALL STATION
ARLINGTON 12, VIRGINIA

Department of Defense contractors must be established for ASTIA services or have their "need-to-know" certified by the cognizant military agency of their project or contract.

All other persons and organizations should apply to the:

U. S. DEPARTMENT OF COMMERCE
OFFICE OF TECHNICAL SERVICES
WASHINGTON 25, D. C.

DESIGN HISTORY AND THEORY OF OPERATION OF A TWO-CHANNEL, ROCKET-BORNE EBERT GRATING SPECTROMETER

by

Merle J. Persky
Eugene K. Dana
Geert Wyntjes

Scientific Report No.
Contract No. AF 19(604)-5738

Project No.
Task No.

January 9, 1963

Prepared for

Geophysics Research Directorate
Air Force Cambridge Research Laboratories
Air Research and Development Command
United States Air Force
Bedford, Massachusetts

Block Associates, Inc.
385 Putnam Avenue
Cambridge 39, Massachusetts

ABSTRACT

This report describes a two-channel Ebert grating spectrometer developed by Block Associates, Inc., under contract number AF 19(604)-5738. The ultraviolet channel scans the 2300 Å to 7000 Å spectral region. The infrared channel scans the 2.3μ to 7μ spectral region. Built-in calibration is provided to monitor the response of the two spectral channels and the operation of the telemetering system. Data commutation is used to time-multiplex the information onto a single channel data link. The system is fully transistorized and both mechanical and electrical design are compatible with rocket-borne environments.

In addition to the design and development history and general design considerations for this type of instrument, information is also presented on the details of operation of the instrument.

LIST OF FIGURES

TABLE OF CONTENTS

1.0 Instrument Specifications

The following is a summary of the specifications of the dual channel spectrometer developed under this contract which has been designated Model E-8.

	IR Channel	UV Channel
Wavelength range	1μ - 4.6μ	2100Å - 6800Å
Output voltage	0 V - 5 V	0 V - 5 V
Dynamic range	100 linear 10^3 log	100 linear 10^3 log
SNEPD (watts $cm^{-2}\mu^{-1}$)	10^{-7}	10^{-10}
Wavelength repeatability	±0.01μ	±5 Å
Wavelength accuracy	±0.02μ	±10 Å
Resolution	0.1μ	50 Å
Monochromator	Ebert-Fastie f/2 60mm.	Ebert-Fastie f/2 60mm.
Grating	30 x 30 mm.	30 x 30 mm.
Slits (curved)		
Entrance	0.012" x 0.950"	0.006" x 0.950"
Exit	0.015" x 0.950"	0.010" x 0.950"
Detector	PbSe	1P28
Power required	1.5 A @ 28 VDC	
Scan rate	1.2/sec (#6)	1.2/sec (#6)
Total field of view, nominal	20° x 20°	20° x 20°
Size	7½" x 6" x 14 5/8"	
Weight	13 lbs.	

2.0 General Theory of Operation

2.1 Optics. The E-8 spectrometer is divided into an ultraviolet channel and an infrared channel. The two channels are functionally similar.

Incident radiation enters the instrument through an appropriate spectral bandpass filter, is chopped, passed through the entrance slit, collimated, and then sent to a dispersion grating. A portion of the incident energy dispersed by the grating will be focused through the exit slit onto the detector.

Each channel divides its spectral region into two separate parts to eliminate order-sorting problems, and scans each region separately. The initial bandpass filters are chosen to coincide with the scanning regions. The filter assembly of each channel contains the two order-sorting filters and a calibration source. The elements of this assembly are programmed through the proper positions to correspond to the desired data cycle. This is designed so that the calibration source in each channel appears every fifth spectral information cycle. The spectrum produced by the calibration light serves to monitor instrument performance during flight.

2.2 Electronics. The detector output (figure 1) is preamplified and then sent to a logarithmic amplifier. The wide dynamic range of the logarithmic amplifier allows the E-8 to operate over a wide range of incident energy levels. The output of the logarithmic amplifier is synchronously rectified and then sent to the commutator.

The commutator receives output spectra from the UV and IR channels, detector and chopper temperature information, and +12 VDC from the power supply. The power supply voltage is divided down to form three reference voltage steps which monitor telemetering-linearity as well as power supply functioning. This

information is commutated into a single output data channel. The output signal is similar to that shown in figure 2. The commutator also programs the calibration lights on and off at the proper time.

2.3 Mechanics. The E-8 contains two motors, figure 1. The d.c. motor operates off 28 VDC to drive the chopper wheel. The a.c. motor operates off 400 cycle power and drives the dispersion grating, the commutator and the filter assembly.

Figure 3 shows an assembly drawing of the E-8. The two optical channels are driven from a common drive train. Electronic assemblies are mounted to permit ready accessibility for service. The subassemblies are mounted directly on the mounting frame which is integral with the mounting flanges. This not only provides rugged construction, but also provides good thermal conduction paths to the missile structure.

3.0 Design History

3.1 Background. The research and development of the E-8 spectrometer was undertaken as an extension of Block Associates' previous experience with the E6 spectrometer. The project was divided into two phases: the first phase was an exploration of various problems associated with high performance spectroscopy; the second phase was the development and construction of an improved spectrometer.

The following areas were explored in the initial phase of the project:

1. Extension of spectral range to cover the ultraviolet.
2. Improved vibration resistance.
3. Optimization of the optical design.
4. Achievement of a highly versatile instrument.
5. Reduction of calibration and manufacturing costs.
6. Weight reduction.

Work in these areas did not cease with the conclusion of phase one, but continued on into phase two. The major difference between the two phases of the project was one of emphasis. Work in phase one was carried out in the context of an exploration of what might be done. Work in phase two was carried out in the context of producing a workable instrument. Thus the design history given below often discusses a problem without specifically mentioning which phase of the work it was done in.

3.2 Optical-Mechanical Design History

3.2.1 Extension of spectral range to cover the ultraviolet. The major problem was the selection and mounting of an appropriate photomultiplier tube. Tubes with a variety of surfaces and windows were tested in order to select a tube with the best combination of the desired qualities - sensitivity, spectral range, small size, and vibration resistance. Selection was eventually

narrowed to the RCA 7105 and the RCA 1P28. The 1P28 was chosen because of its better UV response.

The high sensitivity of the photomultiplier tube necessitated very careful design to minimize stray radiation. Light leakage was minimized by careful packaging design. Internal reflection of spurious wavelengths was minimized by baffling.

3.2.2 Improved vibration resistance. The chassis was stiffened in various ways to give it greater strength. The electronics were mounted on a frame independent of the optical components to provide independent suspension.

The most difficult vibration problems concerned the photomultiplier tube. A detailed theoretical analysis of the vibration behavior of photomultiplier tubes was made and a mounting was designed to permit the tube to operate in the intended vibration environment.

The final mounting configuration utilized a mu-metal shield around the tube to prevent electrical pick-up, with low Durometer rubber pads between the shield and the frame to provide vibration isolation. This configuration was then placed on a shake table. Starting with 1 G, 10-2,000 cycles, the G load was increased until component failure resulted. One of the tube elements eventually broke from metal fatigue at 15 G. There was no evidence of microphonics prior to failure. It is believed that the tube should normally be able to take 20 G loads without failure.

3.2.3 Optical design. The major problem was the attainment of high resolution in a small package. Small size means high f-numbers, forcing an inefficient use of the optical elements. A laboratory model spectroscope utilizing Ebert optics was constructed and extensive testing to optimize the optical parameters was begun.

Using the desired exit slit width, (Appendix I) the proper entrance slit width was established by progressively narrowing it until further decreases only reduced throughput without improving resolution. This was the slit width used in the final configuration.

Finally, the best ratio of entrance to exit slit widths was investigated. Best resolution was obtained when the exit slit was made a few thousandths of an inch wider than the entrance slit. Using less of the grating area also yielded higher resolution.

In the IR channel it was necessary to balance a number of factors. Large throughput and high resolution require the use of curved exit slits. Thus the detector must either be of sufficient size to collect the energy passed through the slits or optical techniques must be used to focus the energy onto a smaller detector. Both of these techniques would tend to reduce sensitivity. A large detector would have a degraded NEP and optics produce losses. Even so the detector must be wide enough to cover all the area behind the exit slit. This was no problem in the UV channel because of the large area of the photomultiplier sensitive surface. However large areas mean low responsivity in infrared detectors. Thus, a detector of sufficient width to cover a curved exit slit would have more area, hence diminished responsivity. The solution of this problem was the development of a thin, curved indium antimonide detector. Use of a curved detector had the additional advantage of making the exit slit unnecessary and thus simplified the optical design.

3.2.4 Production of a highly versatile instrument. The design philosophy here was to produce one standard model spectrometer that could be easily adjusted in the field to provide different scan rates, slit widths, fields of view, spectral

ranges, resolutions and output voltages for varied conditions. Unfortunately, the flexibility goal conflicts with a number of other project goals such as small size, light weight and reliability.

The characteristics of a spectrometer are interdependent. Thus a change in one parameter necessitates changes in the other parameters as well, if optimum spectrometer performance is to be obtained. This greatly complicates the problem of obtaining versatility. For example, changing the spectral region requires a change of filters, detector, biasing, chopping rate, grating, grating cam, input impedance and rectifier time constant.

Electrical flexibility can be obtained by adding extra components and rotary switches. Mechanical flexibility involves changing cams and gear trains and hence produces a whole family of interlocking problems. Neither of these difficulties is insoluble, but their solutions result in a larger, more complex instrument with less reliability in extreme environments. Consequently, the research originally directed toward producing a field-adjusted instrument was redirected toward producing an easily adjustable, factory-adjusted instrument.

3.2.5 Exploration of ways to reduce calibration and manufacturing costs. The major effort here was devoted to designing an instrument that could be easily aligned and calibrated since calibration cost has generally proven to be a very large portion of instrument cost in the past. A number of different optical configurations were experimented with toward this end. These are described in section 3.2.7 below.

Cheaper production of the component parts was also explored. Attempts were made to build mirrors, mountings, chopper blades and other parts out of epoxy. Casting these parts out of epoxy mixed with carbon black would have saved both machining and

anodyzing costs. This had to be given up though, due to aging problems with the epoxy.

3.2.6 Weight reduction. Making a number of the components out of epoxy, which is lighter than aluminum, was tried, but the dimensional stability of epoxy was not high enough for use in our optical system. A light-weight optical design was also tried. This is described in section 3.2.7.

3.2.7 Final design. A number of different designs were tried and three were worked on intensively. The first of these utilized an optical configuration similar to that described in section 4.1.1, below. This configuration has several good features: the motor and the detector are well separated; it is easy to change detectors; and the optics are easily accessible for adjustment. Unfortunately this configuration also has a number of disadvantages: it places the detector too close to the chopper wheel and hence makes it subject to wind noise; it requires a more complex chopper drive; and its overall dimensions must be large to permit mirror adjustment.

The next design that was tried was an I beam configuration. Viewed from the top, the supporting frame was shaped like an I beam. Each channel of the I contained one monochromator. This design has a number of advantages: both monochromators have the same orientation; optical adjustment is simple; only one drive motor is needed; the gear trains are simple; the optical components are easily accessible; and its weight is low due to the simple mechanical configuration. This configuration has one major disadvantage: it is sensitive to vibration. A great deal of work was done to stiffen the construction, but vibration problems with the mirror and grating suspension eventually forced the abandonment of this configuration.

The third configuration tried was the one that is actually being used in the present E-8. It is described in section 4.1.2 below.

3.3 Electronics Design History

3.3.1 IR Preamplifier. Due to the low output of the indium antimonide detector a preamplifier with extremely high gain, low noise and good stability was required. A circuit using three stages of direct-coupled amplification was designed to fulfill these requirements. Both AC and DC feedback were added to stabilize the circuit. To deal with the noise problem the following things were done: the input impedance of the preamplifier was exactly matched to that of the detector; special grounding procedures were used to minimize ground loop problems; the entire preamplifier assembly was electrically and magnetically shielded; the chopper motor was magnetically shielded and special twisted-pair, double-shielded connecting wire was used; the $\pm$ 10 Volt Filter Platter was added to provide ripple-free power.

3.3.2 IR Detector. The indium antimonide detector that was developed and utilized in the E-8 has the disadvantages of microphonics, low impedance, sensitivity to magnetic fields and sensitivity to mechanical strain. Indium antimonide was used in spite of these disadvantages because it was the only material available that could meet the requirement of wide spectral response. To minimize the above-mentioned disadvantages, the detector was enclosed with Mu metal magnetic shielding, securely mounted on a plate rigidly attached to the preamplifier, and the entire assembly suspended by means of shock mounts to isolate it from vibration. The low responsivity necessitated the design of a high gain, low noise preamplifier and the use of three paralleled

calibration bulbs to produce sufficient output.

3.3.3 EA7 Amplifier. This amplifier produces the demodulating voltage used in the Logarithmic Amplifier. The demodulating voltage must be at a precise DC level, its waveform must be exactly symmetrical, and its phase must be adjustable. To assure a proper DC reference level the input bias is precisely set at the factory and a zener diode is connected across the output. A special feedback circuit was designed to automatically adjust the symmetry of the output waveform by varying the input bias.

To achieve a phase adjustable waveform of the proper shape, a system was used in which light from a reference source was interrupted by the chopper wheel and then picked up by an EA7 solar cell. Since the same chopper wheel also controls the energy incident on the IR and UV detectors, proper frequency of the demodulator signal is automatically assured. Proper phase is produced by varying the position of the reference light, which was designed with an adjustable mounting for this purpose.

3.3.4 High Voltage Unit. The major problem encountered was the prevention of corona effects due to the reduced pressures of flight environments. To reduce the number of high voltage leads, the voltage divider resistors were mounted on the base of the photomultiplier tube. The base of the tube was then potted. To eliminate corona around the single remaining high voltage lead, the lead was made continuous with no breaks in the insulation. The High Voltage Unit, itself, was also potted but other difficulties were then encountered due to the potting compound permeating the transformer windings. Potting compound has a higher dielectric constant than air and hence increased the

inter-winding capacitance of the transformer. This problem was corrected through improved potting techniques. Finally, it was discovered that the high voltage line was picking up interference from the DC motor and so a filtering network was added to the base of the photomultiplier tube.

4.0 Detailed Theory of Operation

4.1 Optics

4.1.1 Ebert Optical Systems. Figure 4 shows a typical Ebert mounting. The entrance and exit slits, S_1 and S_2, are both in the focal plane of the spherical mirror M_2. Two baffles, B_1 and B_2, are used to minimize stray light. The focal properties of the system can most easily be understood if the grating, G, is considered as a mirror.

Figure 5 is an equivalent optical diagram. Rays R_1 and R_2 are the extreme rays of the system. They are mirror images of each other and hence their optical paths are equal. Thus the only significant aberration produced by the system will result from astigmatism. Astigmatism is no problem if the entrance and exit slits are short. However, short slits mean low throughput. Higher throughput can be obtained by using long curved slits. This is illustrated in figure 6.

Figure 6 is an end-on view of the optical system. Mirror M_1 is behind the plane of the paper. Mirror M_2 and the two slits lie in the plane of the paper. The axis of the system is at C. Assume the entrance and exit slits are both straight. A short line image of the point b will appear at b'. The line image will be perpendicular to bCb' and hence is not properly focused across the exit slit. When the slits are short this is not a significant problem. Longer slits make it more serious.

Assume the entrance and exit slits in figure 6 are curved. A short line image of a will appear at a'. The short line image will be perpendicular to aCa' and will coincide with the exit slits. Hence by using curved slits, both large throughput and low astigmatism can be obtained.

4.1.2 E-8 Optical System. The Ebert system used in the E-8 functions as follows: incident radiation passes through an order

sorting filter, is then chopped and goes through a curved entrance slit. Radiation from the entrance slit, figure 7, is reflected off a 45° mirror onto the spherical collimating mirror. From the collimating mirror the radiation goes to the dispersing grating and then back again to the collimating mirror to be focused across a curved exit slit onto the photomultiplier tube in the UV channel. The IR channel uses a curved indium antimonide detector and hence does not need an exit slit.

The grating is rocked by a cam assembly, shown in the upper right hand corner of figure 3. The filter assembly, containing the two order-sorting filters and the calibration source, is automatically programmed by a cam arrangement geared to the grating cam shaft.

4.2 Electronics

4.2.1 IR Channel

4.2.1.1 Pre-Amplifier. The output of the IR detector is a chopped wave. This signal goes to a three stage, direct coupled pre-amplifier consisting of Q600, and Q601 and Q602 (see Fig. 9). Negative feedback is taken from the output of Q602 and coupled through R601 and R605 back to the base of Q600. Capacitor C600 eliminates the AC component of the feedback. The connection from the emitter of Q602 to the emitter of Q600 provides AC feedback. The output of the pre-amplifier is coupled through capacitor C602 to the logarithmic amplifier.

4.2.1.2 Logarithmic Amplifier. The logarithmic amplifier is capable of accepting a large dynamic range of input signals -- 5,000:1. It amplifies and rectifies these signals and then delivers them to the commutator. The wide dynamic range is achieved as follows (see Fig. 8): the signal enters amplifier Q800, is amplified, and then split into two parts. One half is

coupled down to the summation line and the other half is amplified in amplifier Q802. The output of Q802 is also split, half going to the summation line and half going on to the next amplifier, Q804. Amplifiers Q804 and Q806 operate the same way. The total signal on the summation line is fed to a DC amplifier, Q808 and Q809, and then out to the commutator.

Assume that the signal entering the logarithmic amplifier from the pre-amplifier is fairly small (Fig. 8). In that case the input will be amplified in four successive stages before entering the operational amplifier. As the input signal becomes larger, amplifier Q806 will eventually saturate. When Q806 saturates, the total gain of the four stages will be reduced. As the input signal increases still more, Q804 will eventually saturate and further reduce the overall gain of the four stages. Thus when the input signal is small the overall gain is high and remains high until the input increases enough to saturate the last stage and lower the overall gain. Further increases in the input cause successive stages to saturate and reduce the overall gain still further. Hence the amplifier can accept inputs with a dynamic range of 5,000:1.

The logarithmic amplifier also functions as a synchronous rectifier. Light from L1000 (figure 8) is chopped and then picked up by the solar cell, EA7. The square wave output of EA7 is amplified and then coupled through transformer T800 to the base of switching transistors Q801, Q803, Q805 and Q807. Thus the switching transistors are alternately cut off and saturated at the same frequency as the amplifier input. During one half cycle, Q801 and Q805 will be cut off and Q803 and Q807 will be saturated. During the other half of the cycle, Q803 and Q807 will be cut off and Q801 and Q805 will be saturated. If

a particular switching transistor is cut off then the signal output from the previous amplifier will be coupled onto the summation line. If the switching transistor is saturated, then part of the amplifier output will be shorted to ground and will not reach the summation line. Since the signal to be amplified goes through a 180° phase shift in each amplifier and at the same time alternate switching transistors are either cut off or saturated, the signals which reach the summation line are all in the same phase. The signal on the summation line is further amplified by the DC amplifier, Q808 and Q809. The time constant of the parallel RC network provides smoothing for the signal.

A more detailed signal flow will now be given. The chopped wave from the pre-amplifier is coupled to the base of Q800, figure 9. The output of Q800 is developed across R800 and coupled through C800, C801, and R811 to the base of Q802. Resistor R808, figure 9, provides negative feedback and diode CR800 is slightly back-biased to provide limiting of the input signal. Capacitors C800 and C801 provide DC isolation. A portion of the output of Q800 is also coupled through R809 and R823 onto the summation line. If switching transistor Q801 is saturated the signal going to the summation line is shunted to ground.

The operation of Q802, Q804 and Q806 is identical to that already described for Q800. The rectified voltage on the summation line is coupled to the base of the DC amplifier Q808 which is wired in a common collector, emitter follower, configuration. The output of Q808 is developed across R820 and is direct coupled to the base of Q809. The output of Q809 is developed across R821 and then coupled through diode CR806 to the commutator. Diode CR805 clamps the DC bias on the collector of Q808 and diode CR806 allows the output signal to pass through, but at the

same time it provides a sufficient DC voltage drop to insure zero output voltage to the commutator when no signal is being received on the base of Q809. Capacitor C808 and resistor R807 are chosen so that their time constant will provide smoothing of the output signal.

The synchronizing voltage from the solar cell, EA7, is amplified and then received on the primary of T800. The secondary of T800 is resistive coupled to the bases of the switching transistors. Diode CR807 is a silicon diode that maintains a constant 6 volt drop across itself. This provides a stable DC bias for the amplifier transistor. Resistor R838 adjusts the back bias on the limiting diodes CR800, CR801, CR802 and CR803 and is set to produce symmetrical clipping.

4.2.1.3 EA7 Amplifier. Light from the reference light, L1000, is interrupted by the blades of the chopper wheel and is received by the solar cell, EA7. The output of EA7 is direct coupled to the base of Q1000, amplified and then direct coupled to the base of Q1001. The output of Q1001 is direct coupled to the base of Q1002, amplified, and then coupled out of the unit through C1001. Since the output of the EA7 Amplifier is used as the demodulation switching voltage in the Logarithmic Amplifiers it is essential that it be symmetrical around the proper reference level. Accordingly, three extra features have been added to the circuit: resistor R1004 is factory selected to produce the proper output reference level; zener diode CR1002 acts to limit the output if it tries to go too far negative; and C1000 acts to keep the output square wave symmetrical about the reference level. Assume that the output square wave became unbalanced in a negative direction. This would cause C1000 to build up a charge and change the bias level on Q1000, which would restore the symmetry of the output. As long as the output is symmetrical, the charge

on C1000 will not change.

4.2.2 UV Channel

4.2.2.1 Pre-Amplifier. The output of the photomultiplier tube is coupled through C102 to the base of Q200. The amplified output of transistor Q200 is developed across R201 and then direct-coupled to the base of Q201. The output of Q201 is developed across R203, R202, and R205 and then coupled through R300 and C300 to the base of Q300 in the logarithmic amplifier. Resistor R200 couples negative feedback to the base of Q200 and resistors R202 and R203 couple negative feedback to the emitter of Q200. Diode CR200 sets the DC bias level on Q201.

4.2.2.2 Logarithmic Amplifier. The operation of the logarithmic amplifier in the UV channel is the same as the operation of the logarithmic amplifier in the IR channel, described in 4.2.1.2 above. These two amplifiers differ only in the input coupling to the first stage.

4.2.3 Power Supplies

4.2.3.1 Convertor and + 12V Regulator Power Supply. Transistors Q1100 and Q1101 act as switches to send DC current alternately up and down in the primary of T1100 and hence induce an AC signal in the secondary. Initially + 20 VDC is coupled to the emitter of each transistor through the primary winding of T1100. Resistor R1100 couples the base of Q1100 to ground and hence causes the base-emitter diode to be slightly forward biased. Transistor Q1100 will thus begin to conduct and cause current to flow in winding 2,3 of T1100. This induces a negative voltage at pin 1 and a positive voltage at pin 5. The induced negative voltage at pin 1 is coupled through R1101 and C1100 to the base of Q1100. This causes Q1100 to conduct even harder, which induces a greater current flow in winding 2,3 and induces a greater

negative voltage at pin 1, which in turn causes Q1100 to conduct harder, and so on. Thus the base of Q1100 is becoming more and more negative and the base of Q1101 is becoming more and more positive. Saturable reactor TC1100 is connected between the bases of the two transistors and hence will have a current flow through it. As the potential difference between the two bases increases, the current flow through TC1100 will increase until it saturates. When TC1100 saturates, the negative bias on Q1100 is coupled over to the base of Q1101 and causes it to start conducting. Conduction by Q1101 causes a current flow through winding 3,4 of T1100, which induces a negative voltage on pin 5 and a positive voltage on pin 1, which drives Q1101 further toward conduction and Q1100 further toward cutoff, and so on. The potential difference across TC1100 is reversed; current flows in the other direction; and eventually it saturates again to reverse the process. Thus TC1100 prevents either transformer winding from ever reaching saturation and acts to time the circuit.

The changing voltage in the primary of T1100 induces a voltage in secondary winding 6,8. Pin 7 is grounded and CR1100 and CR1101 act as a full wave rectifier. Filtering is provided by R1103, R1105 and C1102. Transistors Q1102, Q1103 and Q1104 form a voltage regulator circuit. Assume that the output voltage tries to drift in a positive direction. This positive increase will be coupled by R1107 and C1104 to the base of Q1104. A positive voltage on the base of Q1104 will cause the collector of Q1104 to become more negative. This causes the base of Q1102 to go negative and hence makes the emitter of Q1102 more negative; this makes the base of Q1103 more negative and causes it to conduct more. Greater conduction by Q1102 makes the emitter of Q1102 more negative and hence

cancels out the original positive increase.

The +12 volt regulator, Q1105, Q1106 and Q1107, functions in a similar fashion to the -12 volt regulator described above. Zener diode CR1104 provides a reference source for the +12 volt regulator. Since the reference for the -12 volt regulator is derived from the R1107, R1118, R1117 voltage divider, which is attached to the +12 volt output, CR1104 also acts to provide a reference for the -12 volt regulator.

4.2.3.2 Input Regulator and 400 Cycle Motor Supply. The 28 VDC input on pin 1 is coupled through fuse F900 and diode CR900 to (1) the DC motor, (2) the +18 volt light calibrate supply, and (3) the input regulator. The input regulator is similar to the +12 volt regulator described above.

The 400 cycle convertor is a modification of the ±12 volt converter described above. Instead of a saturable reactor connected between the two bases, the transformer T900 is itself saturable. Resistor R904 serves as the starting resistor and the initial circuit operation is the same as that already described with Q902 driven to conduction and Q903 driven to cutoff. This process is eventually reversed when the field around T900 collapses, a back EMF is generated and Q903 begins conducting. Diodes CR902 and CR903 protect the transistors from these inductive spikes. Capacitor C902 and resistor R906 act to provide additional filtering.

4.2.3.3 High Voltage Unit. The +12 volt input is coupled through R510 to the center tap of the primary of T500. The -12 volt input is regulated by Q502 and Q503 (see description of the ±12 volt convertor-regulator above) and then coupled to the collectors of Q500 and Q501. Transistors Q501 and Q502 form an alternate switching circuit similar to the one in the ±12 volt

converter, described above. The output of T500 is rectified and doubled by CR500, CR501, C500, C501, and C502. The resultant +1200 volts is coupled through R500 to the photomultiplier tube.

4.2.3.4 +18 Volt Calibrate Light Supply. This unit receives 28 volts and sends out a regulated +18 volt supply to power the calibration lights. Any drift in output voltage is coupled through C1200 and R1203 to the base of Q1203. Zener diodes CR1200 and CR1201 provide an exact reference voltage. The circuit is similar to the +12 volt regulator circuit described above.

4.2.3.5 ±10 Volt Filter Platter. This unit receives ±12 volt inputs and reduces and regulates them to produce ±10 volt outputs for the IR preamplifier. Transistors Q700 and Q701 perform the regulation and zener diodes CR700 and CR701 act as reference sources.

Appendix I: Design of Fastie-Ebert Optical Systems

1. General Considerations. Figures 10 and 11 show the general appearance and design parameters of a Fastie-Ebert optical system. This appendix sets forth the design calculations for a system scanning the .23-.70μ and the 2.3-7.0μ spectral regions. If it is desired to use the instrument in a different spectral region, the same procedure can be used to calculate the necessary changes.

2. Calculation Procedure, IR Channel. The initial step is to determine the first-order grating scan that will be used. The spectral region of interest is 2.3μ to 7μ. If a grating scan was chosen to cover this entire region it would have the following higher-order scans:

1st order scan	----	2.3μ to 7.0μ
2nd order spectrum	----	$\frac{2.3\mu}{2}$ to $\frac{7.0\mu}{2}$ or 1.15μ to 3.5μ
3rd order spectrum	----	$\frac{2.3\mu}{3}$ to $\frac{7.0\mu}{3}$ or 0.766μ to 2.33μ
4th order spectrum	----	$\frac{2.3\mu}{4}$ to $\frac{7.0\mu}{4}$ or 0.575μ to 1.75μ

It can immediately be seen that the upper-end of the 2nd order spectrum will overlap the lower-end of the 1st order scan and hence cause ambiguity in signal interpretation. Thus only the wavelengths from 3.5-7.0μ should be allowed to reach the detector during the 1st order scan. A filter could easily be inserted into the field of view to accomplish this. However, the 1st order scan still covers the 2.3-7.0μ region. Thus we are wasting one-quarter of the 1st order scan. To get around this inefficiency the 1st order scan should be designed to cover only the 3.5-7μ region. This would give the following higher order scans:

1st order scan ---- 3.5μ to 7.0μ

2nd order spectrum ---- $\frac{3.5\mu}{2}$ to $\frac{7.0\mu}{2}$ or 1.75μ to 3.5μ

3rd order spectrum ---- $\frac{3.5\mu}{3}$ to $\frac{7.0\mu}{3}$ or 1.18μ to 2.33μ

4th order spectrum ---- $\frac{3.5\mu}{4}$ to $\frac{7.0\mu}{4}$ or 0.87μ to 1.75μ

The 2nd order spectrum no longer interferes with the 1st order scan, and neither do any of the higher orders. The 3rd order spectrum does interfere with the 2nd order spectrum though. The only solution to this is to waste some of the 2nd order spectrum. The final scan regions and order-sorting filters are shown below:

SCAN	REGION	ORDER-SORTING FILTER
1st order	3.5μ to 7μ	3.5μ to 7μ
2nd order	1.75μ to 3.5μ	2.33μ to 3.5μ
3rd order	1.17μ to 2.33μ	NOT USED

The instrument will now scan 2.33μ to 7.0μ, using two scans and two order-sorting filters. The 1.75μ to 2.33μ portion of the 2nd order spectrum is being wasted, but that portion of the scan time can be used to telemeter instrument calibration information, and thus make full use of the instrument's duty cycle.

Once the 1st order scan is determined, equation (A) is used to determine the angle through which the grating must rock and, consequently, the rise of the cam.

$$\sin \phi = \frac{n \lambda}{2 d \cos c/2} \qquad (A)$$

where ϕ = angle between the optical center line and the normal to the grating

n = order

λ = wavelength, m.m.

d = grating spacing, m.m.

c = included optical angle, 66° (a constant for all wavelengths; determined by "A", the radius of the slit measured from the optical center line, and the focal length)

See figures 10 and 11.

Substituting into equation (A) for a wavelength of 3.5μ we get

$$\sin \phi = \frac{1\ (3.5\mu \times 10^{-3}\ \text{m.m./}\mu)}{2\ (1/_{150})\ \text{m.m.}\ \cos \frac{66°}{2}}$$

$$= \frac{.0035\ \text{m.m.}}{(1/_{75})\ \text{m.m.}\ (.83867)}$$

$$= .315$$

and $\phi = \underline{18.4°\ \text{at}\ 3.5\mu}$

Substituting into equation (A) for a wavelength of 7.0μ we get

$$\sin \phi = \frac{1\ (7.0\mu \times 10^{-3}\ \text{m.m./}\mu)}{2\ (1/_{150})\ \text{m.m.}\ \cos 33°}$$

$$= .630$$

and $\phi = \underline{39.1°\ \text{at}\ 7.0\mu}$

Therefore the grating must rock through an angle from 39.1° to 18.4°, or a 20.7° angular motion.

The resolution of the instrument at the wavelength λ is

$$\text{Res.}\ \lambda = (\text{R.L.D.}\ \lambda)\ (\text{exit slit width}) \qquad (B)$$

where R.L.D. λ is the Reciprocal Linear Dispersion $(\frac{\Delta \lambda}{L})$ calculated from equation (C).

$$\text{R.L.D.}\ \lambda = (\frac{d}{nf})\ \cos\ (\frac{c}{2} + \phi) \qquad (C)$$

where f = focal length, m.m.

The R.L.D. at 3.5μ will be

$$\text{R.L.D.}\ \lambda = (\frac{1/150\ \text{m.m.}}{1 \times 60.88\ \text{m.m.}})\ \cos\ (33° + 18.4°)$$

$$= \frac{1}{9132}\ (.62388)$$

$$= 6.82 \times 10^{-5}\ \text{m.m.}/_{\text{m.m.}}\ \text{at}\ 3.5\mu$$

The R.L.D. at 7μ will be

$$\text{R.L.D.}\,\lambda = \frac{1}{9132}\cos(33° + 39.1°)$$

$$= 3.36 \times 10^{-5}\ \text{m.m.}/\text{m.m.}\ \text{at } 7\mu$$

For an exit slit width of 0.015", the resolution of the instrument at 3.5μ can be calculated from equation (B).

$$\text{Res.}\,\lambda = (6.86 \times 10^{-5})\ (.015 \times 2.54 \times 10^{4}) = \underline{0.026\mu \text{ at } 3.5\mu}$$

$$= \underline{0.0128\mu \text{ at } 7.0\mu}$$

It is important to note that the resolution figures just calculated are for an optically perfect Fastie-Ebert system. In practice the resolution is limited by imperfections such as: error in the optical figure of the mirror, slit imperfection, errors in the ruling of the grating, and aberration from using the spherical mirror so far off axis - this last imperfection probably being the most important one.

The grating used in the IR channel has a spacing of 150 lines per m.m. Consistent with availability of commercial gratings, the blaze wavelength of the grating is chosen to fall at the center of the 1st order scan, 5.25μ in this case. Grating efficiency seems to fall off equally on both sides of the blaze wavelength but there is little information available on this point.

Figure 12 illustrates the field of view of the system. Notice that the portion of the spherical mirror used, M, is constant but that the effective width of the grating, W, will vary as a function of grating angle. Figure 13 is an equivalent diagram of the optical system. The field of view, β, is determined by the mirror focal length, f, and the parameter G. The distance G is determined by the size of M and W; it is equal to whichever of them is smaller.

Assume that the grating is positioned so that W is at maximum width and that M is not limiting the field of view. The parameter G will then equal W, which is the size of the grating, and the field of view is

$$\beta = 2 \tan^{-1} \frac{G/2}{f}$$

$$= 2 \tan^{-1} \frac{30 \text{ m.m.}/2}{60.88 \text{ m.m.}}$$

$$= 2 \tan^{-1} \frac{15}{60.88}$$

$$= 2 \ (14°)$$

$$= 28° \text{ maximum field of view}$$

Present information indicates that neither the length nor width of the entrance slit should effect the field of view. Since the grating is square and the spherical mirror is not a limiting factor, the instrument must have the same maximum field of view in both dimensions. The field of view will always be 28° in one dimension, but it will vary in the other dimension as the grating rocks back and forth and W changes.

If any fore-optics are used, they become the limiting factor on instrument field of view. This is shown in figure 14. With a slit width of .015" and an objective lens with a 2.0" focal length we get

$$\beta = 2 \tan^{-1} \frac{S/2}{f}$$

$$= 2 \tan^{-1} \frac{0.015/2}{2.0}$$

$$= 2 \ (\tfrac{1}{4}°)$$

$$= \tfrac{1}{2}° \text{ field of view}$$

3. Calculation Procedure, U.V. Channel. The spectral region of interest is 0.23μ to .70μ. With a 1st order scan of 0.35μ to 0.70μ, the following higher orders will result:

1st order scan	----	0.35μ to .70μ
2nd order spectrum	----	0.175μ to 0.35μ
3rd order spectrum	----	0.117μ to 0.233μ
4th order spectrum	----	0.0875μ to 0.175μ

To cover the region of interest, two scans and two order-sorting filters will be necessary. The final scan regions and order-sorting filters are shown below:

SCAN	REGION	ORDER-SORTING FILTER
1st order	0.35μ to 0.70μ	0.35μ to 0.70μ
2nd order	0.175μ to 0.35μ	0.233μ to 0.35μ
3rd order	0.117μ to 0.233μ	NOT USED

Given the 1st order scan, we can now calculate ϕ from equation (A). For a wavelength of 0.35μ we get

$$\sin \phi = \frac{1 \ (0.35\mu \times 10^{-3} \text{ m.m./}\mu)}{2 \ (1/600) \text{m.m.} \cos \frac{66°}{2}}$$

$$= \frac{0.105}{0.83867} = 0.125$$

and $\phi = \underline{7.2° \text{ at } 0.35\mu}$

at a wavelength of 0.70μ we get

$$\sin \phi = \frac{1 \ (0.70\mu \times 10^{-3} \text{ m.m./}\mu)}{2 \ (1/600) \text{m.m.} \cos 33°}$$

$$= \frac{0.21}{0.83867} = 0.251$$

and $\phi = \underline{14.5° \text{ at } 0.70\mu}$

Therefore the grating must rock through an angle from 14.5° to 7.2°, or a 7.3° angular movement.

The R.L.D. λ at 0.35μ can be calculated from equation (C).

$$\text{R.L.D.}\lambda = \left(\frac{1/600 \text{m.m.}}{1 \times 60.88 \text{ m.m.}}\right) \cos (33° + 7.2°)$$

$$= \frac{1}{36,528} \quad (0.7638)$$

$$= 2.092 \times 10^{-5} \text{ m.m./}_{\text{m.m.}} \text{ at } 0.35\mu$$

And R.L.D. λ at 0.70μ will be

$$\text{R.L.D.}\,\lambda = \left(\frac{1/600}{1 \times 60.88}\right) \cos(33^\circ + 14.5^\circ)$$

$$= \frac{1}{36{,}528} \quad (.6756)$$

$$= 1.85 \times 10^{-5} \text{ m.m.}/_{\text{m.m.}} \text{ at } 0.70\mu$$

And from equation (B) we can calculate the expected resolution with .010 exit slits for each wavelength

$$\text{Res.}\,\lambda = (2.092 \times 10^{-5})\ (0.01 \times 2.54 \times 10^{4})$$

$$= \underline{0.0053\mu \text{ at } 0.35\mu}$$

$$\text{Res.}\,\lambda = (1.85 \times 10^{-5})\ (0.01 \times 2.54 \times 10^{4})$$

$$= \underline{0.0047\mu \text{ at } 0.70\mu}$$

The calculation for field of view of the U.V. channel is identical to that already done for the IR channel since the two optical systems have the same dimensions.

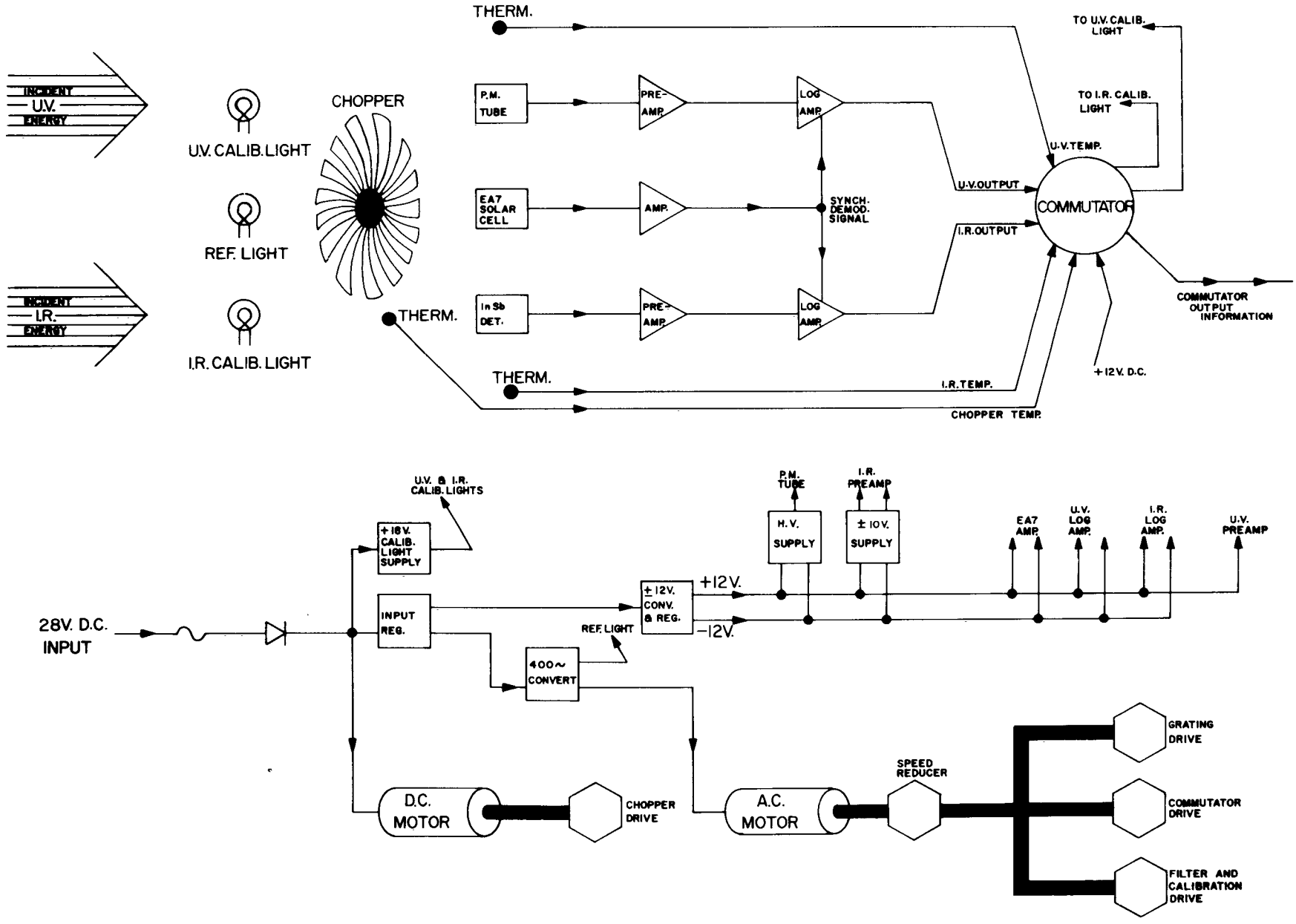

E8 BLOCK DIAGRAM

FIG. 1

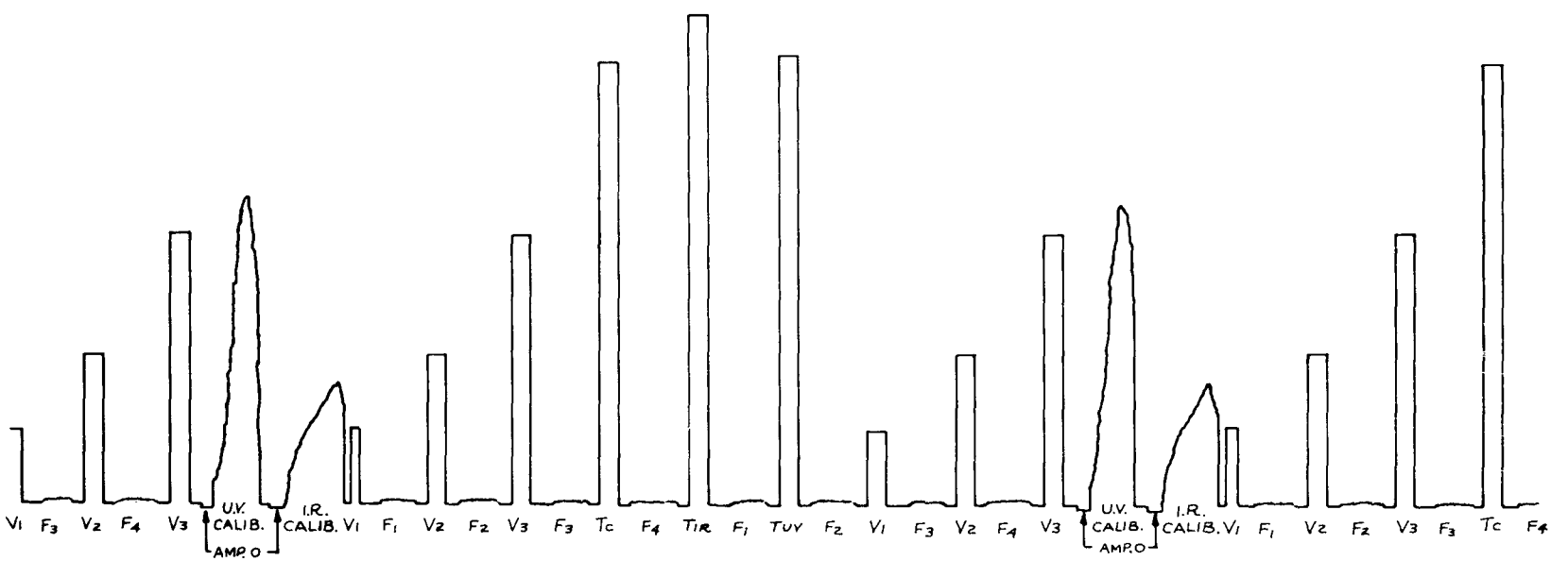

F_1 = 2300 - 3500 Å
F_2 = 7000 - 3500 Å
F_3 = 2.3 - 3.5 μ
F_4 = 7.0 - 3.5 μ

T_c = CHOPPER TEMP.
T_{IR} = IR DETECTOR TEMP.
T_{UV} = UV DETECTOR TEMP.

$V_1 \approx 1.5V.$
$V_2 = 3.0V.$
$V_3 \approx 4.5V.$

FIG. 2

Block Associates, Inc.
CAMBRIDGE, MASSACHUSETTS

PROJECT	E 8-8		
TITLE	OUTPUT WAVE SLOPE		
MATERIAL	NO REQ.	SCALE	ASSEM. USED IN
DRAWN A.D. DATE 9/20/62	CHECKED DATE		APPROVED BY
UNSPECIFIED TOLERANCES DECIMALS FRACTIONS ANGULAR ± .005 .015 ±1° 0	DWG. NO. B-89-185 REV. 0		

REVISIONS DO NOT SCALE DWG. – BREAK CORNERS & SHARP EDGES

A-60

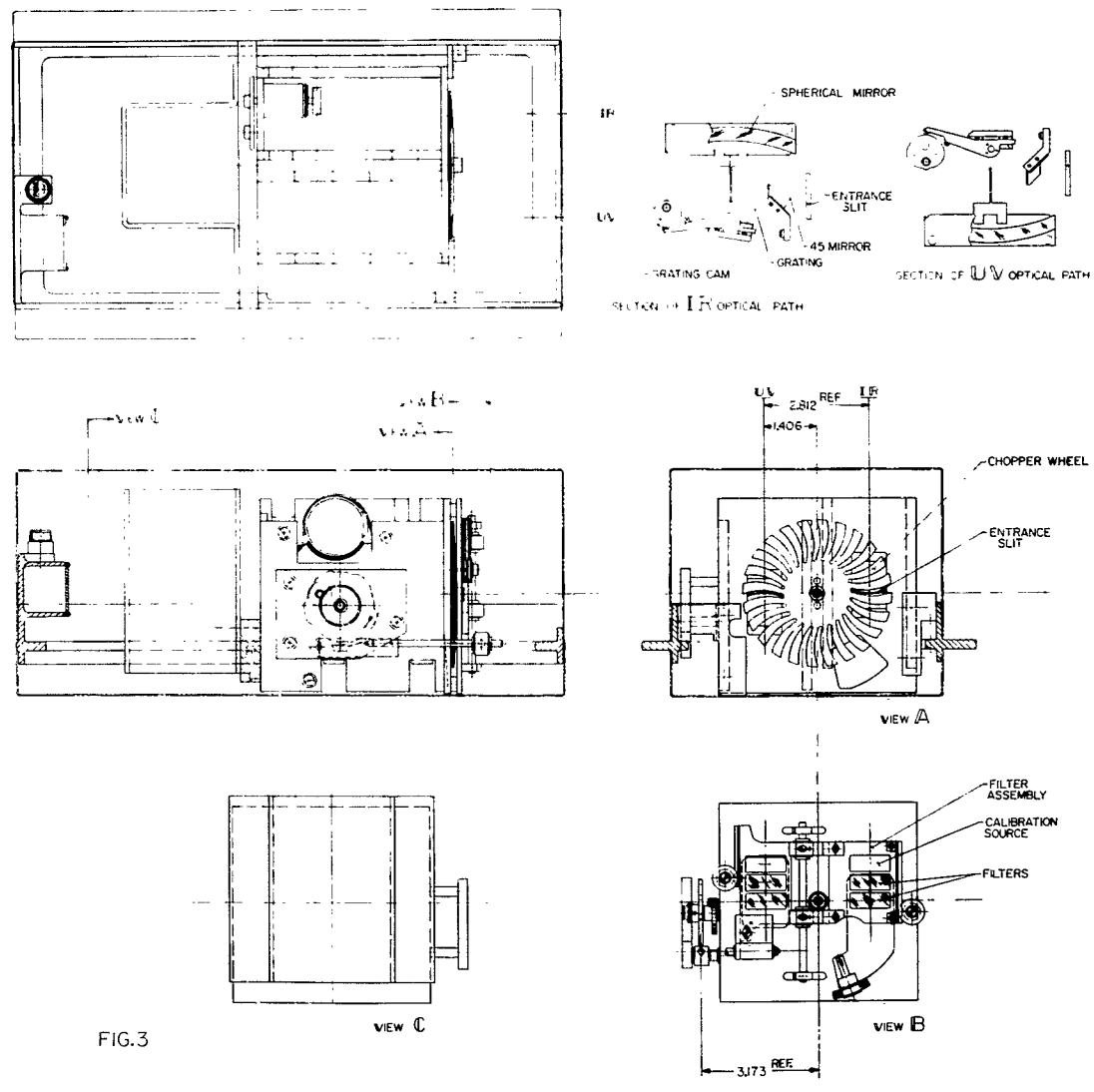
IR
UV
SPHERICAL MIRROR
ENTRANCE SLIT
45 MIRROR
GRATING
GRATING CAM
SECTION OF UV OPTICAL PATH
SECTION OF IR OPTICAL PATH
VIEW C
UV
2.812 REF
IR
1.406
CHOPPER WHEEL
ENTRANCE SLIT
VIEW A
FILTER ASSEMBLY
CALIBRATION SOURCE
FILTERS
VIEW B
3.173 REF

FIG.3

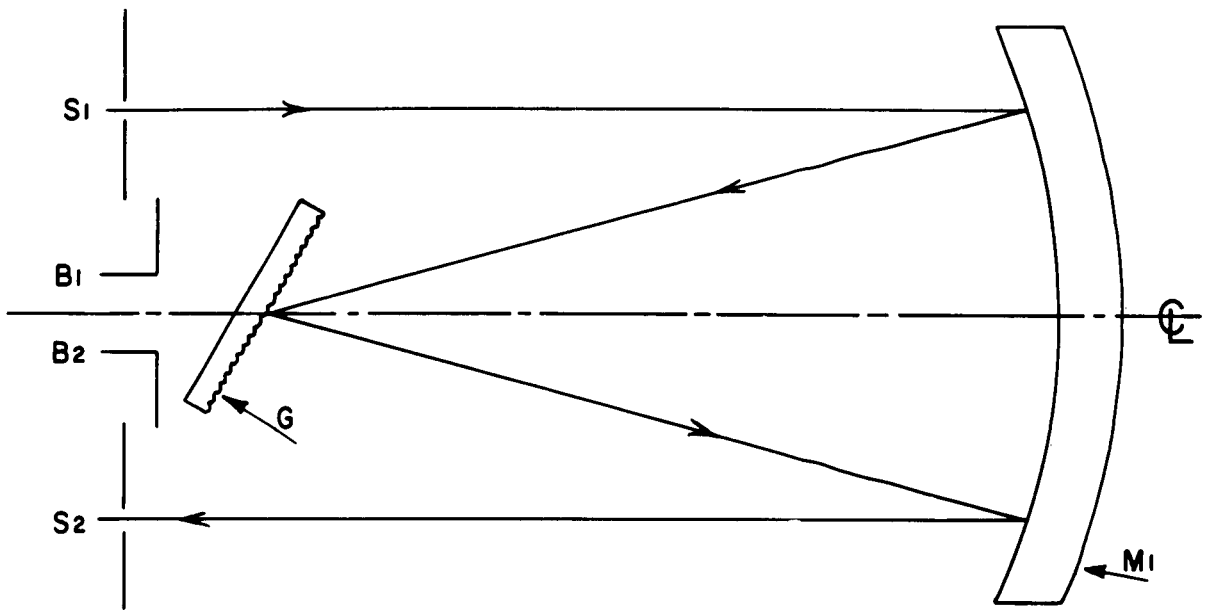

FIG. 4

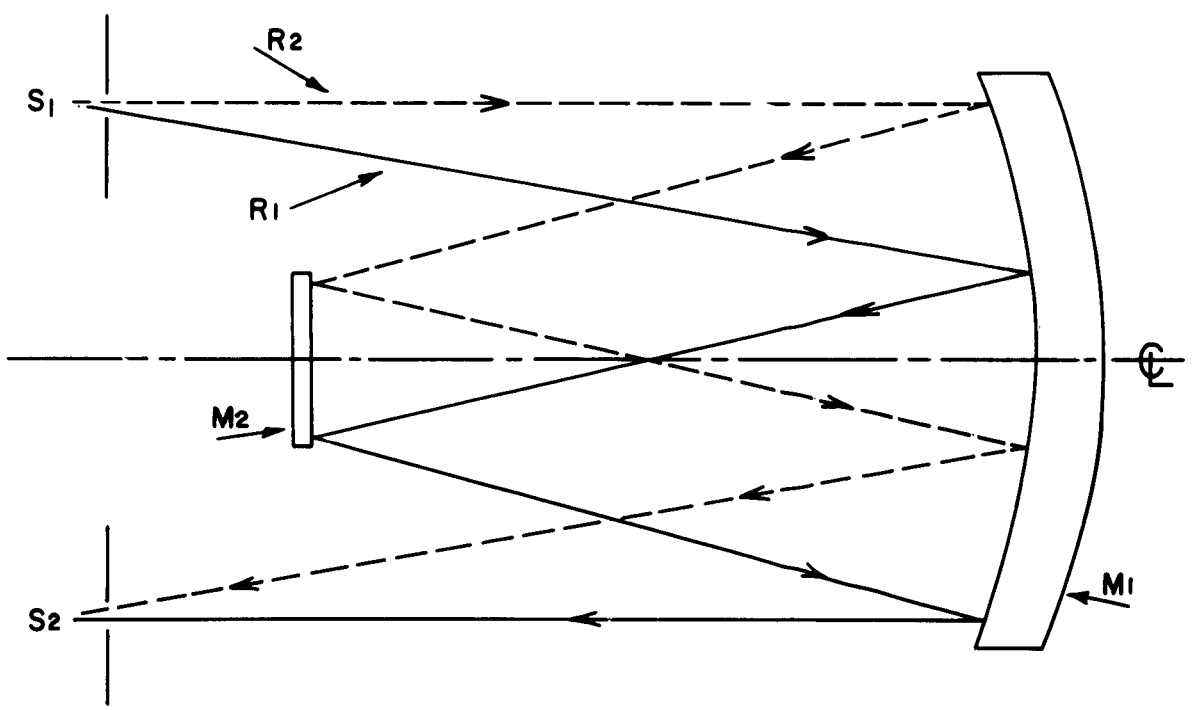

FIG. 5

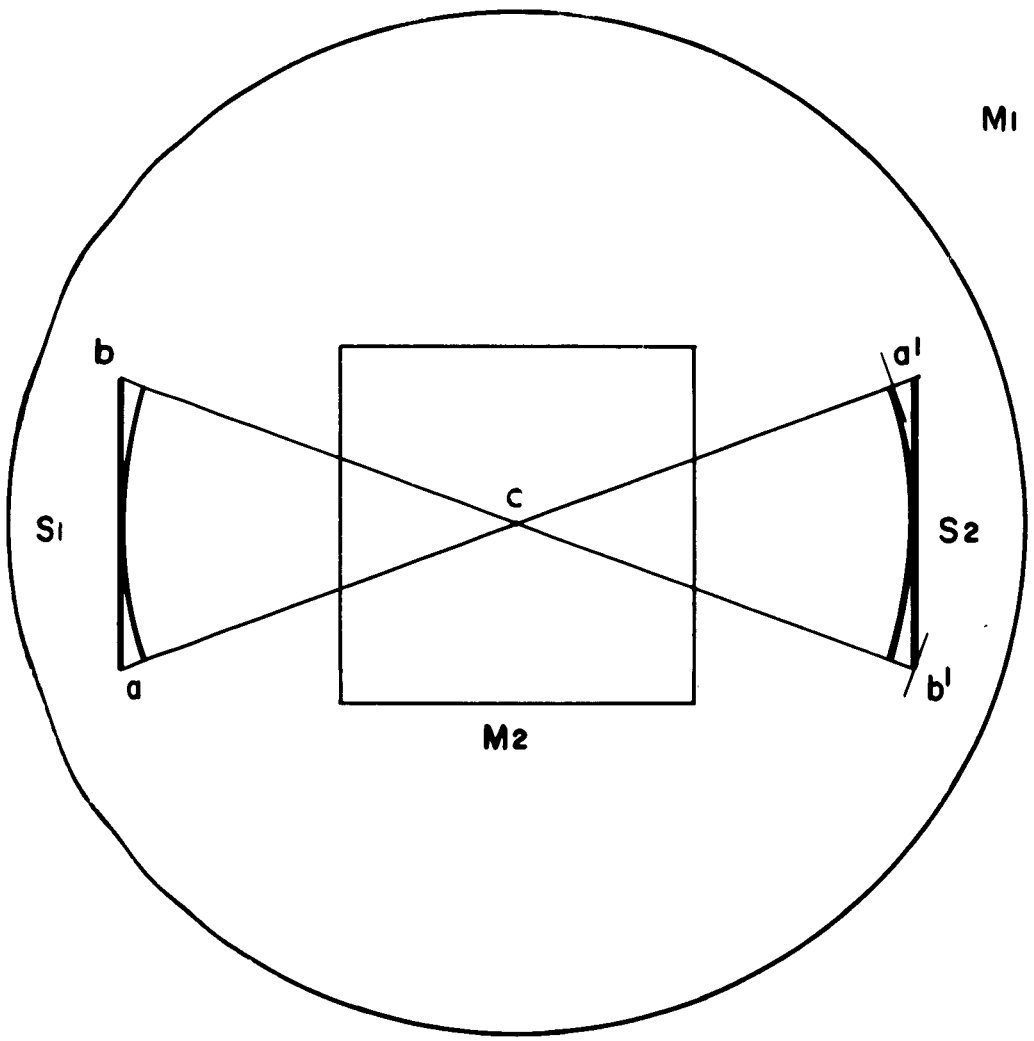

FIG. 6

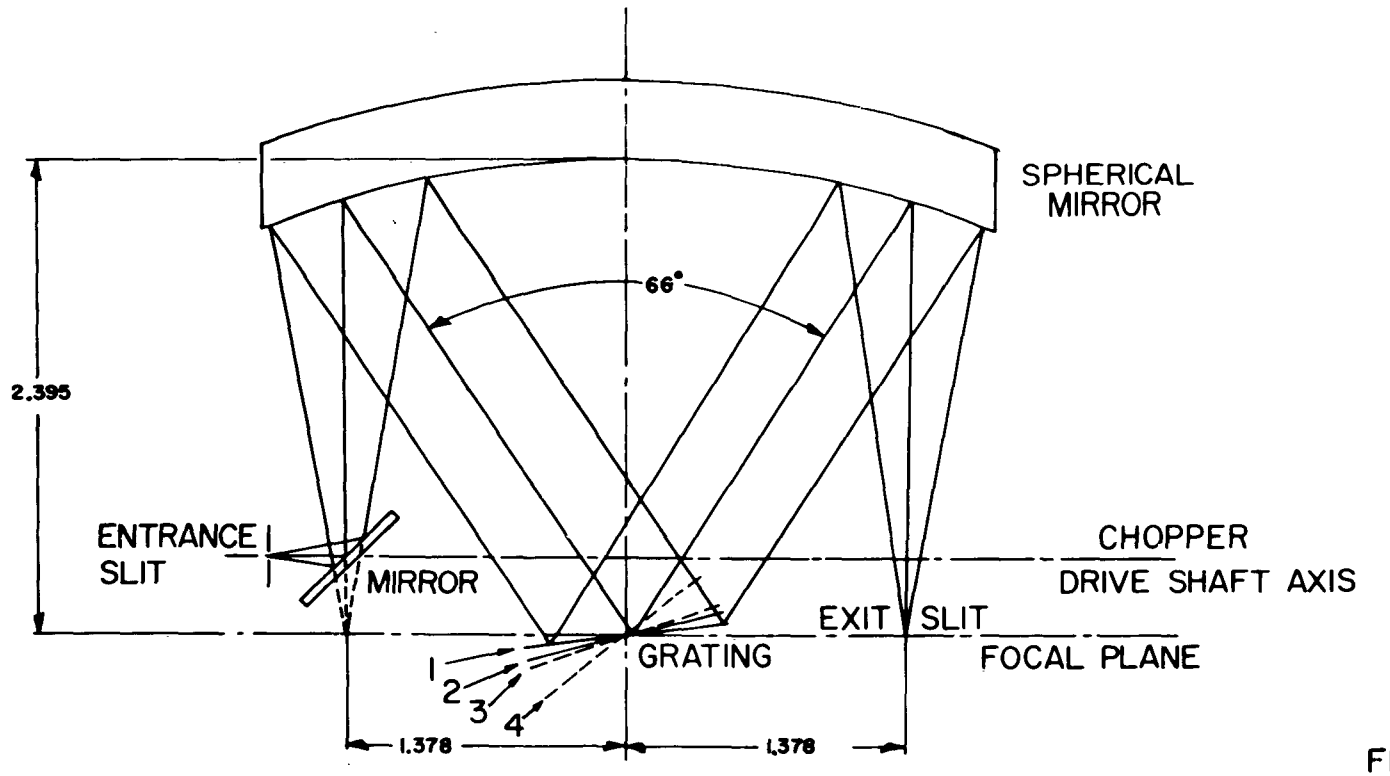

FIG.7

1-6.987°
2-14.504°
3-18.244°
4-38.765°

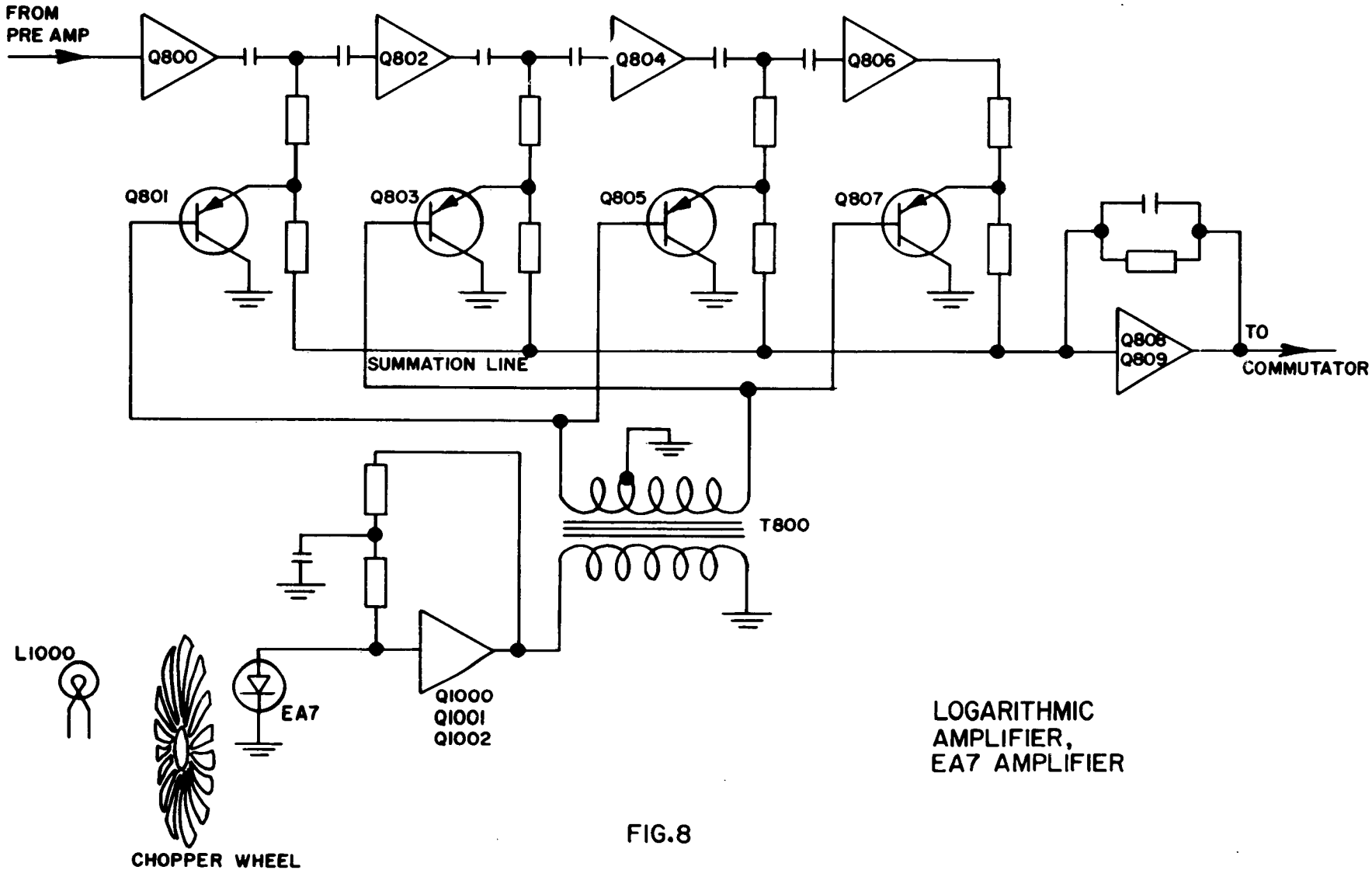

LOGARITHMIC
AMPLIFIER,
EA7 AMPLIFIER

FIG.8

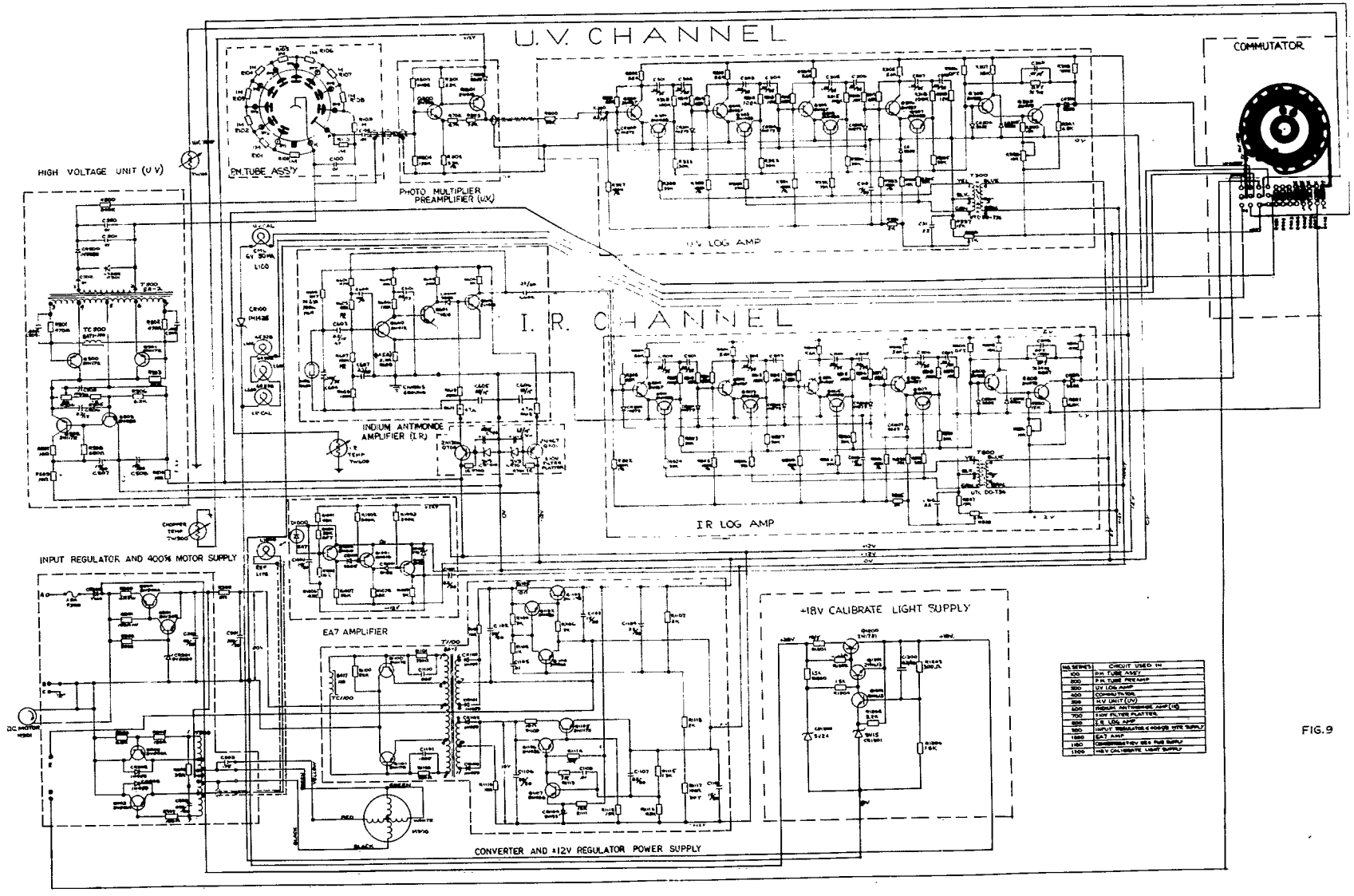
U.V. CHANNEL
I. R. CHANNEL
COMMUTATOR
HIGH VOLTAGE UNIT (U V)
PM TUBE ASSY
PHOTO MULTIPLIER PREAMPLIFIER (U.V.)
U.V. LOG AMP
INDIUM ANTIMONIDE AMPLIFIER (I.R.)
I.R. LOG AMP
INPUT REGULATOR AND 400% MOTOR SUPPLY
EA7 AMPLIFIER
+18V CALIBRATE LIGHT SUPPLY
CONVERTER AND ±12V REGULATOR POWER SUPPLY

FIG.9

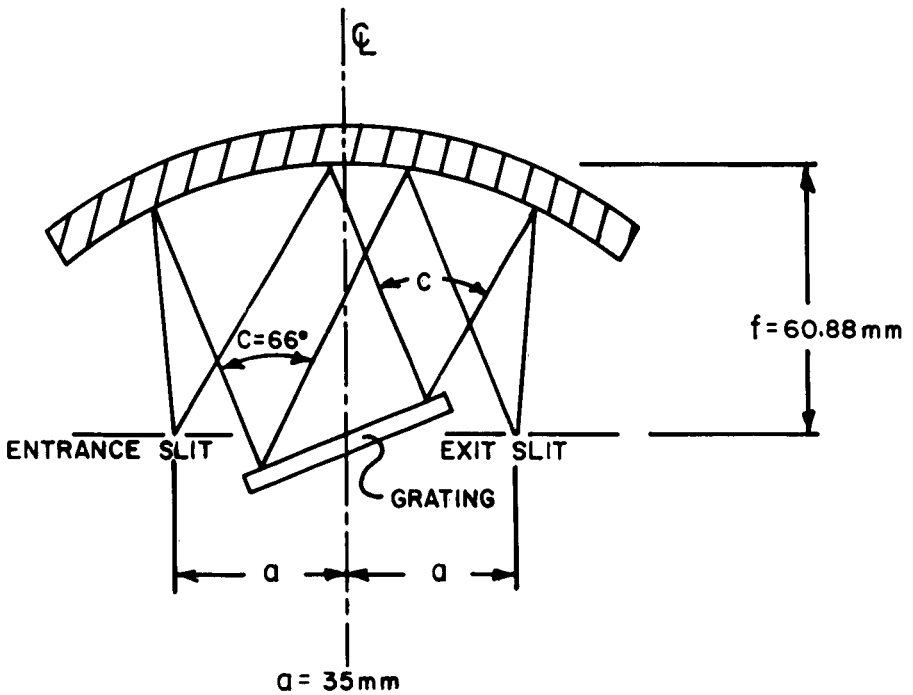

FIG. 10 OPTICAL SYSTEM PARAMETERS

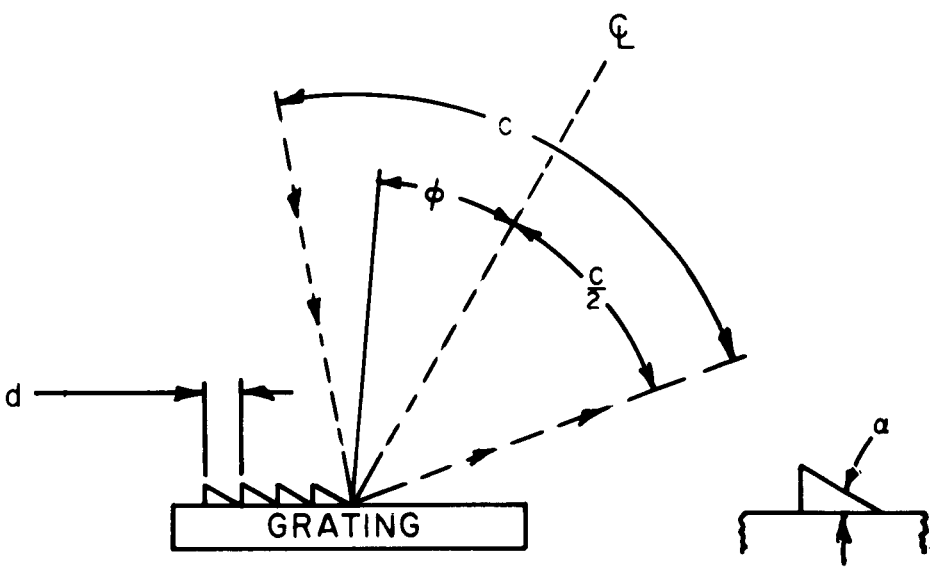

FIG. 11 GRATING PARAMETERS

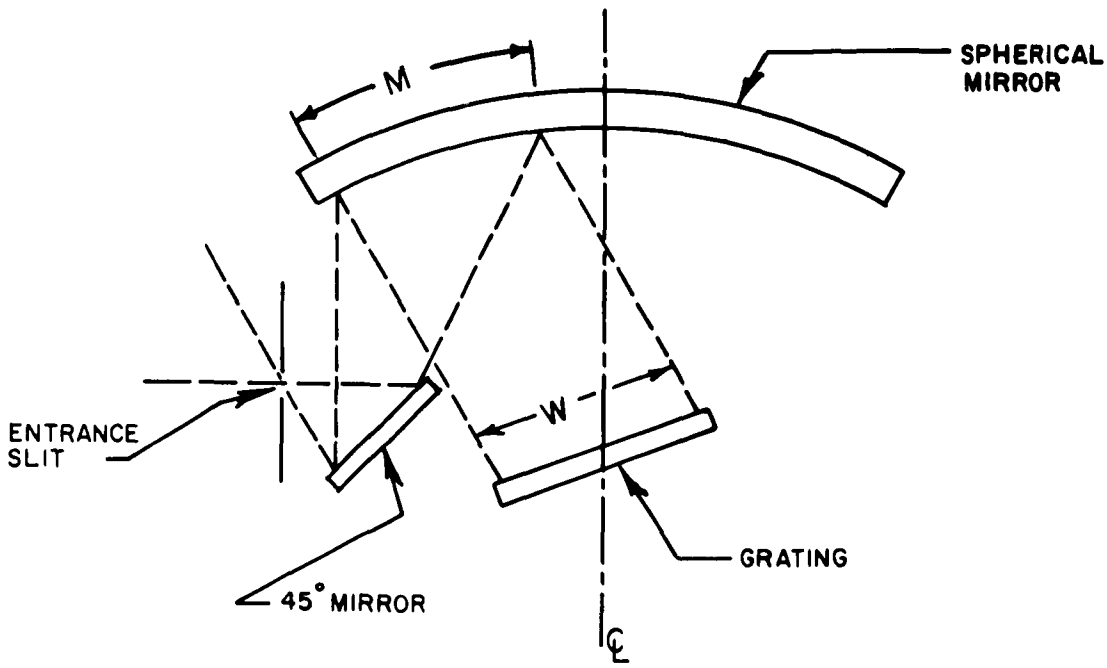

FIG. 12 SYSTEM FIELD OF VIEW

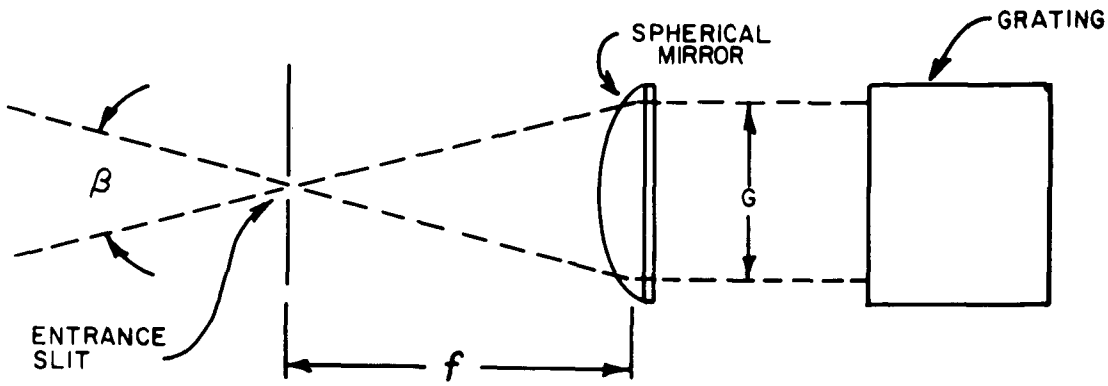

FIG. 13 FIELD OF VIEW CALCULATION

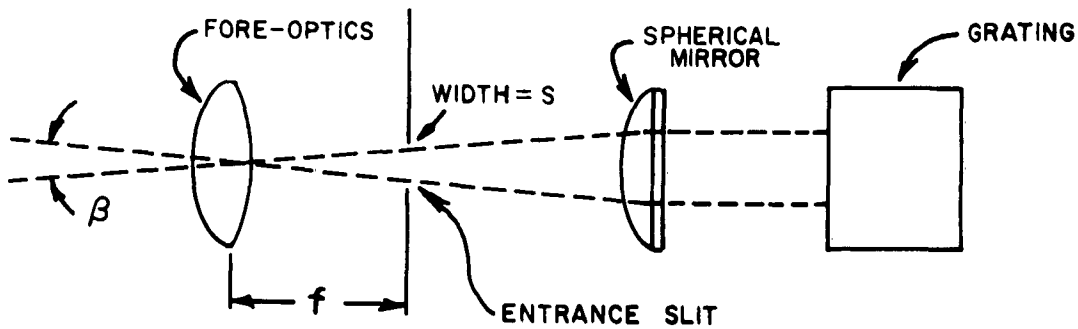

FIG. 14 FIELD OF VIEW CALCULATION WITH FORE-OPTICS